Astronomy Reports, Vol. 39, No. 5, 1995, pp. 587 - 593. Translated from Astronomicheskii Zhurnal, Vol. 72, No.5, 1995, pp. 660 - 667.

Expanding Shells in the Galaxy HoII: Comparison of Numerical Simulation with Observational Data

S. Ya. Mashchenko and S. A. Silich

Main Astronomical Observatory, Ukrainian Academy of Sciences, Goloseevo, Kiev, 252127 Ukraine

Received September 24, 1994

Abstract – Numerical simulation of the evolution of expanding HI shells in the irregular dwarf galaxy HoII, which is a member of the M81 group, were conducted. The results are compared with the HI distribution obtained with the VLA. Inconsistencies between the expected and observed directions of elongation of many shells is connected with the effect of local inhomogeneities in the interstellar medium and with interaction between the shells. A simple method allowing discrimination between the two possible orientations of the angular-momentum vector for the galaxy rotation is suggested.

1. INTRODUCTION

The detection of large-scale cellular structure in the interstellar medium (ISM) [1 - 4] lead to the revision of many established ideas about energy release mechanisms and gas dynamics in galaxies. The development of a dynamic model of the ISM regulated by powerful local energy sources served as a powerful stimulus for the development of new hydrodynamic methods [5 - 10] and for investigation of the overall circulation of matter in galaxies [11, 12].

The development of an observational instrumental base – most notably, large radio telescopes and specialized out-of-atmosphere platforms – resulted in a qualitatively new stage in ISM studies, in which the investigation of the gas distribution and dynamics in nearby galaxies can be done with the same spatial resolution as was done previously in our Galaxy. Studies of nearby galaxies are of great importance, since they allow us to avoid problems with selection effects and distance uncertainties, and to obtain a general picture of the spatial distribution of gas in galaxies of various types.

The data on the structure of the ISM diffuse component in our Galaxy have been reviewed by Kulkarni and Heiles [13, 14]. Bochkarev [15] has summarized the studies of our closest surroundings – the region of the Galaxy within 150 - 200 pc from the Sun (the Local Interstellar Medium). Brinks and Bajaja [3] and Deul and Hartog [4] obtained the HI distribution in the nearest massive disk systems similar to our Galaxy – the galaxies M31 and M33. Deul and Hartog [4] attempted to detect molecular gas emission in the ^{12}CO lines from the interior of four large "holes" in the neutral-hydrogen distribution of M33. The upper limit obtained for the molecular gas mass is considerably lower than the HI mass deficiency in the regions studied.

Puche *et al.* [16, 17] set up a program for the study of neutral gas in dwarf galaxies, in order to search for differences in the structure of the ISM in large spiral and low-mass irregular galaxies. Izotov *et al.* [18] undertook spectral observations of the ionized ISM in compact blue galaxies to search for objects with powerful outflows of matter. Studies of the neutral components of the ISM in nearby galaxies have been reviewed by Brinker [19].

Thus, the data obtained thusfar permit conduction of more detailed comparison of theoretical models with the actual distribution of gas in nearby galaxies and the drawing of conclusions about the dynamics of the ISM in these galaxies and the adequacy of existing theoretical models to describe the properties of the real ISM.

In the work presented here, we have performed numerical simulations of the evolution of expanding HI shells in the irregular dwarf galaxy HoII. The results are compared with certain statistical properties of HI-deficient regions observed in this galaxy. In our opinion, the discrepancies found are due to the effect of local inhomogeneities in the interstellar gas distribution (such as large diffuse clouds) or to the interaction of neighboring expanding shells.

In Section 2, we present the parameters of the galaxy HoII that are necessary for the calculations. In Section 3, we briefly describe the numerical scheme used in the calculations. In Section 4, we compare the results of the calculations with the observations, and discuss the HI-deficient region statistical properties that follow from our numerical model and the observations. Finally, in Section 5 we formulate the main conclusions of this work.

1063-7729/95/3905-0587$10.00 © 1995 МАИК Наука /Interperiodica Publishing

2. THE GALAXY HoII

HoII (UGC 4305) is an irregular dwarf galaxy belonging to the M81 group, which is at a mean distance of 3.2 Mpc from our Galaxy. The analysis of the mass distribution in the galaxy cannot be complete without detailed photometry. However, analysis of the rotation curve and of the general properties of HoII allow estimation of the total mass of the gravitationally bound system as $M_{tot} \approx 2 \times 10^9 M_\odot$ [16]. The maximum radius of the visible galaxy radius is 7.5 kpc, and the rotation velocity corresponding to this distance is $V_{rot}(7.5\ \text{kpc}) = 35$ km/s (Fig. 1). From the integrated flux in the 21-cm line, the total mass of neutral hydrogen is $M_{HI} = 7 \times 10^8 M_\odot$. Taking into account helium, the gas mass is $9.3 \times 10^8 M_\odot$, reaching roughly 50% of the total galaxy mass. The heavy-element content in HoII is $\zeta = 0.4$. Puche *et al.* [16] obtained the radial distribution of HI. The characteristic scale of gas distribution inhomogeneity in the Z coordinate was estimated from the gas velocity dispersion and density of matter in the galaxy disk; for a gaussian density distribution in Z

$$n(r, z) = \frac{N(r)}{H\sqrt{2\pi}} \exp\left(-\left(\frac{z}{\sqrt{2}H}\right)^2\right), \qquad (1)$$

this scale is $H = 625$ pc [16]. Here, $N(r)$ is the column density distribution along the galactic radius corrected for the galaxy inclination. It will be possible to construct a more detailed picture of the distribution of gas in the galaxy after detailed photometry is obtained.

Analysis of the velocity field by means of the method of Begeman [20] permits determination of the dynamic center, position angle P.A., and inclination i of the galaxy. For HoII, these parameters are $\alpha = 08^h14^m06^s$, $\delta = 70°52'00''$ (1950.0), P.A. = 177°, $i = 40° \pm 5°$.

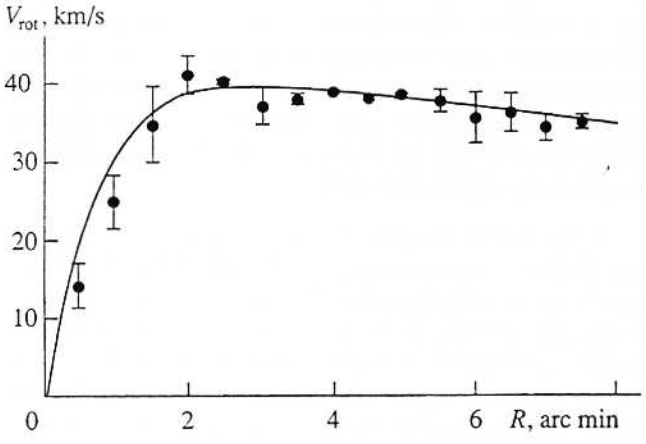

Fig. 1. Rotation curve of the galaxy HoII. The dots are observations, while the solid line is a King model approximation to the observations.

VLA observations [16] detected 51 regions deficient in neutral hydrogen in HoII with sizes ranging between 100 and 1700 pc, which may be considered to be expanding shells or the result of previous evolution of shells. In the centers of some such regions there are massive young stars. HI-deficient regions are also seen in H_α emission. Regions of ionized hydrogen lie at the outskirts of the largest shells and fill all the interior of smaller "holes". This enables us to interpret the objects observed as the result of the collective effect of massive stars belonging OB associations on the surrounding gas.

3. THE NUMERICAL SCHEME

In our calculations, we used the 2.5-dimensional scheme developed by Bisnovatyi-Kogan and Silich [21, 22], based on a thin-layer approximation. The algorithm was modified to take into account thermal-conduction effects, which lead to evaporation of the inner layers of the cool dense shell, establishment of power-law radial distributions of temperature and density, and increase in energy losses due to radiation of this gas [23 - 25]. We modelled the evaporation rate of a non-spherical shell [6] as

$$\dot{M}_{in} = \frac{4}{25} \frac{\mu_i C}{k} T_c^{5/2} \sum_j \frac{d\Sigma_j}{r_j}, \qquad (2)$$

where $\dot{M}_{in}$ is the mass evaporating from the shell per unit time; μ_i is the mean mass per particle of the plasma (if the helium fractional number density is 10%, $\mu_i = \frac{14}{23} m_p$, m_p is the proton mass); the thermal conductivity is taken to be $\kappa = CT^{5/2}$ ($C = 6.2 \times 10^{-7}$ erg/s cm $K^{7/2}$); k is the Boltzmann constant, T_c is the temperature at the shell center; $d\Sigma_j$ and r_j are the area of a shell Lagrangian element and its distance from the shell center. The cooling function $\Lambda(T)$ was modelled using the analytic expression

$$\Lambda(T) = 6.2 \times 10^{-19} \zeta T^{-0.6}, \qquad (3)$$

which, in the temperature range 10^5 - 10^7 K, differs from numerical values [26] by a factor of no more than 2. In (3), ζ is the metallicity. We also took into account energy losses due to ionization of the evaporating matter.

We used a King gravitational model [27] to model the galaxy rotation curve $V(r)$ and the Z component of

the gravitational field g_Z:

$$V(r) = \left(\frac{GM_c}{r_c}\right)^{1/2} \times \left\{\frac{\ln\left[\frac{r}{r_c} + \left(1 + \left(\frac{r}{r_c}\right)^2\right)^{1/2}\right]}{r/r_c} - \left(1 + \left(\frac{r}{r_c}\right)^2\right)^{-1/2}\right\}^{1/2}, \quad (4)$$

$$g_Z = -GM_c\frac{z}{\omega^3} \times \left\{\ln\left[\frac{\omega}{r_c} + \left(1 + \left(\frac{\omega}{r_c}\right)^2\right)^{1/2}\right] - \frac{\omega}{r_c}\left(1 + \left(\frac{\omega}{r_c}\right)^2\right)^{-1/2}\right\}, \quad (5)$$

where G is the gravitational constant, $r = (x^2 + y^2)^{1/2}$ is the cylindrical radius, and $\omega = (x^2 + y^2 + z^2)^{1/2}$ is the spherical radius. We found the King model parameters M_c and r_c from a least squares fit of the calculated to the observed rotation curve. For HoII, these parameters are (Fig. 1):

$$M_c = 1.179 \times 10^9\, M_\odot, \quad r_c = 929 \text{ pc}.$$

The radial distribution $N(r)$ of gas in the galaxy was interpolated from the table given in [16]. We assumed a gas temperature distribution

$$T(z) = (6000 \text{ K})\frac{n(r, 0)}{n(r, z)}. \quad (6)$$

In all calculations, the initial shell radius was 50 pc. We determined the initial thermal energy, coordinates, and velocities of the shell elements from the analytic solution of Weaver *et al.* [25]:

$$U_0 = 0.6\left(\frac{125L_0}{154\pi\rho_0}\right)^{1/5} t_i^{2/5}, \quad (7.1)$$

$$E_{t0} = \frac{5}{11}L_0 t_i, \quad (7.2)$$

$$t_i = \left(\frac{154\pi\rho_0 R_e}{125L_0}\right)^{1/3}, \quad (7.3)$$

where L_0 is the energy input rate to the cavity from supernova explosions, ρ_0 is the unperturbed gas density near the shell center, and U_0, E_{t0}, and R_e are the expansion velocity, thermal energy, and shell radius, respectively, at the initial time t_i.

Our calculations yielded coordinates, velocities, and column densities of Lagrangian elements representing various parts of the moving shell. To compare the numerical results with observations, it is necessary to find the HI projected column density distribution (including the shell and the surrounding galactic gas). Because of the large thickness of the galactic gas layer, it is not possible to approximate the shell as a simple geometric body, such as a cylinder or sphere; and in order to compare the model with observations, it was necessary to numerically project the shell onto the image plane.

To perform this projection it is necessary to change from the galactic coordinates (x, y, z) to coordinates connected with the image plane (x', y', z'). We introduce these frames in such a way that their centers coincide with the dynamic center of the galaxy, and the X and X' axes coincide with a line of nodes and are directed toward the receding edge of the galaxy. We direct the Z axis along the angular momentum vector for the galactic rotation, and the Z' axis along the line of sight. Then

$$\begin{aligned} x' &= x, \\ y' &= y\cos i' + z\sin i', \\ z' &= -y\sin i' + z\cos i', \end{aligned} \quad (8)$$

where i' is the angle between the Z and Z' axes. The angle i' is equal to either the galaxy inclination angle i (which lies between 0° and 90°) or $i' = 180° - i$, depending on the direction of the angular momentum vector of the galaxy. In our calculations, we assumed $i' = i$, i.e., that the angular momentum vector was inclined toward the observer.

The column density along an arbitrary line of sight is the sum of contributions from the shell and the gas

$$N(x', y') = \sum_{j=1}^{m} \frac{N_j}{|\cos\xi_j|} + \int n(x', y', z')dz', \quad (9)$$

where m is the (even) number of intersections between the line of sight and the shell. The integral on the right-hand side of (9) is taken along those sections of the line of sight that lie outside the shell-bounded cavity. We find the HI column density N_j in the corresponding Lagrangian element by numerical simulation of the shell motion. The angle ξ_j is that between the normal to the jth Lagrangian element and the Z' axis ($0° \le \xi_j \le 180°$). From (9) it follows that $N(x', y') \longrightarrow \infty$ for $\xi_j \longrightarrow 90°$. This is a consequence of simulation of a shell with an infinitely thin layer. To exclude this effect, we assumed the ratio $N_j/|\cos\xi_j|$ for areas in which $60° < \xi_j < 120°$ to be as if the angle ξ_j were 60°. This somewhat arbitrary simplification allows smoothing of

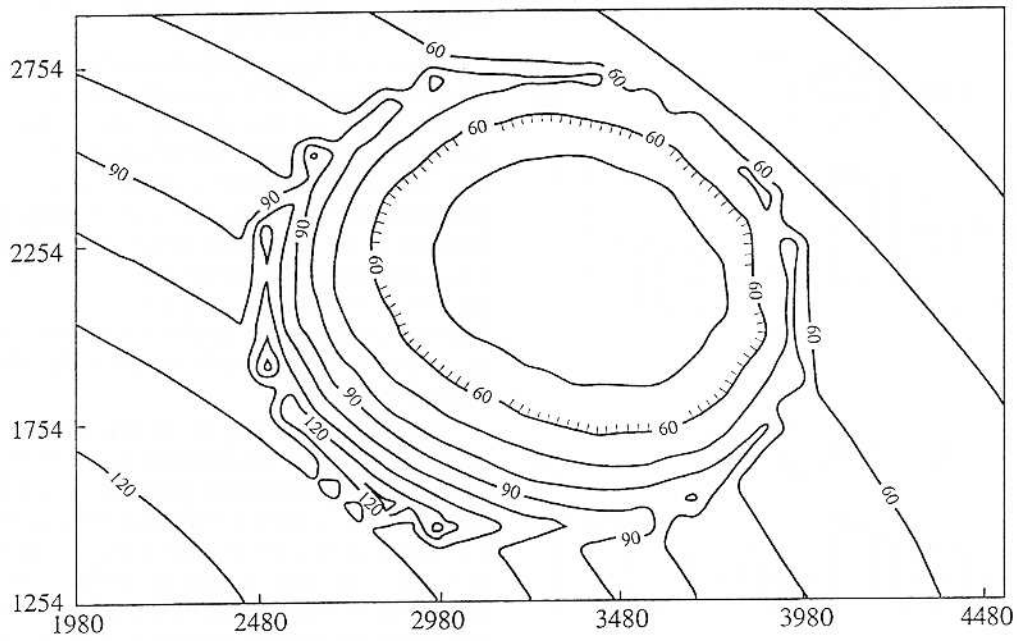

Fig. 2. Contours of equal neutral hydrogen column density around a shell at $R = 4.17$ kpc from the galactic center. The age of the shell is $t = 40 \times 10^6$ years and the angle $\theta = 40°$. Column densities are in units 10^{19} cm^{-2}.

the column density distribution near the shell tangential points and does not affect the main conclusions of this work.

By means of formula (9), we calculated $N(x', y')$ toward the center of every Lagrangian element (in total 1600 areas) and in the shell neighborhood. With these values for $N(x', y')$, we drew contours of the HI column density in the image plane. Figure 2 shows a typical map of the density contour obtained by the method described above. The question arises: which contour should be considered the boundary of the "hole" in the HI column density distribution? The point is that in the galaxy HoII the characteristic scale of inhomogeneities in the unperturbed gas distribution is comparable to the sizes of large shells. As a result, the parts of the shell that lie closer to the galactic center can, when projected, yield contours that are not closed. Therefore, we determined the boundary of the HI-deficient region as follows. We searched for the closed contour connected with the shell that had maximum column density N_{max}. This contour corresponds to the hydrogen density near the shell boundary at the far side from the galactic center. Then we introduced the contrast level $\kappa = 0.1$ and constructed a contour corresponding to the column density

$$N = N_{max}(1 - \kappa). \tag{10}$$

We considered this contour to be the boundary of the hydrogen-deficient region. The closed curve obtained was approximated as an ellipse using a least squares fit. We then calculated the angle φ (see Fig. 3) between the direction toward the galactic center in the image plane and the ellipse major axis

$$\varphi = \delta - \beta', \tag{11}$$

where δ is the angle between the ellipse major axis and the X' axis and β' is the polar angle of the ellipse center in the image plane (in the x', y' frame).

4. DISCUSSION

Numerical simulations of shell evolution were performed for three galactocentric distances: 1.5, 4.17, and 6 kpc. In all cases, we placed the initial OB association in the galactic plane. We assumed that successive supernova explosions provided a quasi-continuous input of energy into the cavity [28] at a rate $L = 3.4 \times 10^{37}$ erg/s over 30 million years, which corresponds to the explosion of approximately 30 supernovae during the lifetime of the OB association.

For comparison with observations, we projected the shells onto the image plane at various polar angles θ, which determined the position of the OB association in the galactic plane. For shells initiated by OB associations at 1.5 kpc from the center, we carried out the projection every 10 million years with the angle θ taking the values $-90°, -80°, \ldots, 80°, 90°$. For this galactocentric distance, the calculations were conducted to 70 million years. After approximately 40 million years, the velocity of individual Lagrangian elements with respect to the unperturbed gas becomes lower than the sound velocity in the ambient gas. These elements then continue their motion in a "flow-around" mode; they do not accumulate the gas flowing in, but only change the

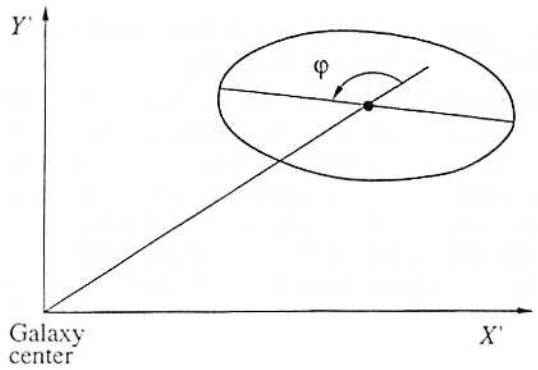

Fig. 3. Schematic presentation of the shell projection onto the image plane.

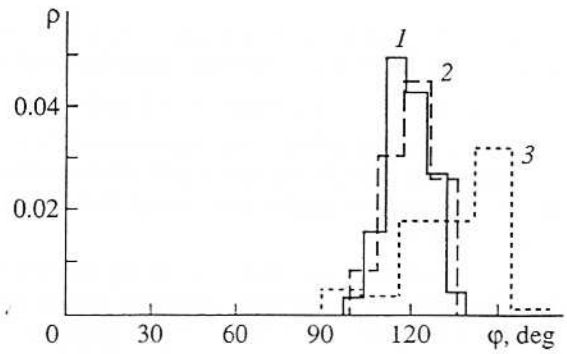

Fig. 4. Normalized distribution density of the distribution of angles φ. Histograms *1*, *2*, *3* correspond to the shells at R = 1.5, 4.17, and 6 kpc, respectively.

normal component of its momentum. Starting at this time, the shell thickness begins to increase at a characteristic rate equal to the sound velocity inside the shell. We stopped the calculations when the shell thickness increased by ~6 - 8% of its radius, and assumed the gas temperature inside the shell to be 1000 K. In this time, the sizes of the "holes" in the HI column density distribution in the image plane reached 1200 - 1500 pc.

For galactocentric distances R = 4.17 and 6 kpc, we performed the projection every 20 million years for the same set of angles θ, and stopped calculations after 80 million years. In this way, we obtained 285 shell "images".

Our aim was to analyze the orientations of the major axes of the ellipses approximating the column density distributions. For nearly circular "holes" with axis ratio $b/a > 0.9$, the reliability of observational determination of the ellipse major axis position angle is doubtful; and we therefore excluded such objects from further consideration.

Figure 4 presents the results of the calculations in the form of histograms for each of the three galactocentric distances. Here, $\rho = \Delta n/(n\Delta\varphi)$ is the density normalized to unity of the shell projection distribution in angle φ, n is the number of the shell "images" obtained for a given galactocentric distance, Δn is the number of shell projections for which the angle φ falls in the interval Δφ. Figure 4 shows that galactic differential rotation stretches the shells in such a way that all the angles φ (Fig. 3) are in the interval $90° < \varphi < 180°$, i.e., the major axes of the "holes" in the HI distributions fall into the I and III quadrants. Remember that the calculations were performed for the case in which the vector of the galaxy rotation angular momentum is inclined toward the observer ($i' = i$). For the other possible direction of the angular momentum vector ($i' = 180° - i$), the major axes of the ellipses fall into the II and IV quadrants ($0° < \varphi < 90°$).

In this way, numerical calculations result in an elementary method allowing determination of the direction of the angular momentum vector in those galaxies for which a statistical analysis of the orientations of the HI-deficient regions is possible. In the case when the angles φ between the straight lines connecting the galaxy center with the HI-deficient region centers and the major axes of ellipses approximating the boundaries of these regions concentrate in the interval $0° < \varphi < 90°$, the galaxy rotation angular-momentum vector is inclined away from the observer. Otherwise ($90° < \varphi < 180°$), the angular-momentum vector is inclined toward the observer. (For galaxies with a greater inclination angle i, the distribution of angles φ may be more complicated.) Note that a deviation of the major axis of the cross-section of the shell and the galactic plane from the normal to the radius vector drawn from the galaxy center to the shell center was found earlier in two-dimensional [29, 30] and three-dimensional [22] calculations.

For the galaxy HoII, we can readily calculate the angle φ from the data given in [16]:

$$\varphi = \text{P.A.}_c - \beta + 90°, \tag{12}$$

where P.A._c is the position angle of the ellipse major axis, and β is the polar angle of the center of the HI-deficient region. The origin of coordinates is fixed at the center of the galaxy, and the Y' axis is directed to the north. We calculated the angles φ for 44 shells from the catalog of Puche *et al.* [16]. We excluded from the analysis seven shells with axes ratios $b/a > 0.9$. The table lists the numbers of objects for which the angle φ falls into the intervals $0° < \varphi < 90°$ and $90° < \varphi < 180°$.

We now consider the statistical hypothesis that the distribution of the observed angle φ in the two equal intervals [0°, 90°] and [90°, 180°] is uniform. To test this hypothesis, we use a χ^2 criterion [31]. For this purpose, we calculate the quantity

$$y = \frac{4}{n}\left(n_1 - \frac{n}{2}\right)^2, \tag{13}$$

where n is the total number of objects analyzed and n_1 is the number of shells with angle φ in the interval

[0°, 90°]. For $0 < R < 3.4$ kpc, $n = 23$, and for $3.4 < R < 7.48$ kpc, $n = 21$. Comparison of this quantity with the tabular value $\chi^2_{1-\alpha}(m-1)$, where $m = 2$ is the number of degrees of freedom, allows determination of the confidence level α at which we can reject the hypothesis that the distribution of angles φ between two contiguous quadrants is uniform.

It follows from the table that there is no statistically significant anisotropy in the distribution of angles φ for the collection of shells observed ($n = 44$). However, for the outer parts of the galaxy with $R > 3.4$ kpc, the hypothesis that the distribution of angles φ is uniform must be rejected at a confidence level of 95%, and the excess of angles φ falling into the interval [0°, 90°] is statistically significant.

In the inner part of the galaxy ($R < 3.4$ kpc), the hypothesis that the distribution of angles φ is uniform can be rejected only at a confidence level of 70%, so that there is no statistically significant excess of angles in either of the two intervals [0°, 90°] and [90°, 180°]. This conclusion contradicts the results of the numerical simulation of supershell evolution, presented in Fig. 4. What is the reason for this discrepancy? We consider that the lack of anisotropy in the distribution of φ in the inner parts of the galaxy may be due to the following reasons. Inside $R = 1.5$ pc, the galactic rotation curve is close to that of a solid-body (Fig. 1), which leads to a reduction of the effects of differential rotation and strengthening of the relative contribution of local inhomogeneities in the gas distribution, such as extended diffuse clouds or the coronae of giant molecular clouds, in which the OB associations now observed were formed [32]. In addition, in the heavily populated central parts of the galaxy, collisions of adjacent shells with each other are more probable. In the smallest systems, this leads to the formation of a single giant cavity in the central part of the galaxy [17].

The anisotropy in the distribution of elongation of HI-deficient regions found for the outer parts of the galaxy HoII is evidence that the galactic rotation angular-momentum vector is inclined away from the observer. Determination of the spin direction of HoII based on analysis of the dust-lane arrangement in this galaxy [33], however, gives the opposite spin direction ($i' = 43° \pm 8°$). This contradiction indicates that either the determination of the near and far sides of HoII from the dust distribution is uncertain, or there is some physical cause suppressing the effect of differential rotation on the shell morphology in this galaxy.

Results of application of the χ^2 criterion to the observed shells

Galactocentric distances of shell centers, kpc	Number of shells with $0° < \varphi < 90°$	Number of shells with $90° < \varphi < 180°$	y	α
0 - 7.48	24	20	0.36	0.45
0 - 3.4	9	14	1.09	0.70
3.4 - 7.48	15	6	3.86	0.95

Our analysis leads to the conclusion that there is strong inhomogeneity of the interstellar medium in the disk of the galaxy HoII on the order of a few hundred. Thus, giant expanding shells can be a kind of probe allowing us to make some general conclusions about the structure of the interstellar medium and the direction of the angular-momentum vector of the galaxy studied.

5. CONCLUSION

(1) We have conducted numerical simulations of the evolution of giant shells expanding under the influence of successive supernovae explosions in the irregular dwarf galaxy HoII. We constructed an algorithm that yielded "images" of three-dimensional shells as HI column-density distributions projected onto the image plane. We compared the results of numerical calculations with the observational data.

(2) The results of the numerical calculations suggest a simple method of discrimination between the two possible directions of the angular-momentum vector of the galactic rotation, based on analysis of the orientation of HI-deficient regions in the image plane. Our analysis gives evidence that the angular-momentum vector for the galaxy HoII is directed away from the observer.

(3) When comparing the calculations with the observational data, there is a discrepancy between the expected and observed directions of elongation of many shells. We consider the main causes of this discrepancy to be local inhomogeneities of the interstellar medium, such as extended diffuse clouds or the coronae of giant molecular clouds, as well as interaction between neighboring shells.

(4) It is necessary to further develop theoretical models of the evolution of shells in the interstellar medium. This will enable us to account for inhomogeneities in the interstellar gas on various scales and for interaction between expanding shells.

ACKNOWLEDGMENTS

The authors thank G.S. Bisnovatyi-Kogan for useful comments and discussion. This work was partially supported by the National Space Agency of the Ukraine, Section 3 (Science-Aimed Space Systems) of the National Space Research Program, and also by grant UC9000 of the International Science Fund.

REFERENCES

1. Heiles, C., *Astrophys. J.*, 1979, vol. 229, p. 533.
2. Heiles, C., *Astrophys. J., Suppl. Ser.*, 1984, vol. 55, p. 585.

3. Brinks, E. and Bajaja, E., *Astron. Astrophys.*, 1986, vol. 169, p. 14.
4. Deul, E.R. and Hartog, R.H., *Astron. Astrophys.*, 1990, vol. 229, p. 362.
5. Tomisaka, K. and Ikeuchi, S., *Publ. Astron. Soc. Jpn.*, 1986, vol. 38, p. 697.
6. MacLow, M.-M. and McCray, R., *Astrophys. J.*, 1988, vol. 324, p. 776.
7. MacLow, M.-M., McCray, R., and Norman, N.L., *Astrophys. J.*, 1989, vol. 337, p. 141.
8. Bisnovatyi-Kogan, G.S., Blinnikov, S.I., and Silich, S.A., *Astrophys. Space Sci.*, 1989, vol. 154, p. 229.
9. Igumentshchev, I.V., Shustov, B.M., and Tutukov, A.V., *Astron. Astrophys.*, 1990, vol. 234, p. 396.
10. Tenorio-Tagle, G., Rozyczka, M., and Bodenheimer, P., *Astron. Astrophys.*, 1990, vol. 237, p. 207.
11. Tenorio-Tagle, G. and Bodenheimer, P., *Annu. Rev. Astron. Astrophys.*, 1988, vol. 26, p. 145.
12. Mashchenko, S.Ya. and Silich, S.A., *Astron. Zh.*, 1994, vol. 71, p. 237.
13. Kulkarni, S.L. and Heiles, C., *Interstellar Processes*, Hollenbach, D.J. *et al.*, Eds., Dordrecht: Reidel, 1987, p. 87.
14. Kulkarni, S.L. and Heiles, C., *Galactic and Extragalactic Radio Astronomy*, Verschuur, G.L. *et al.*, Eds., New York: Springer, 1988, 2nd ed., p. 95.
15. Bochkarev, N.G., *Mestnaya Mezhzvezdnaya Sreda* (The Local Interstellar Medium), Moscow: Nauka, 1990.
16. Puche, D., Westpfahl, D., and Brinks, E., *Astron. J.*, 1992, vol. 103, p. 1841.
17. Puche, D. and Westpfahl, D., *Astrophys. J.*, 1994, (in press).
18. Izotov, Yu., Guseva, N., Lipovetsky, V., and Kniazev, A., *Panchromatic View of Galaxies: Their Evolutionary Puzzle*, Hensler, G. *et al.*, Eds., Paris: Frontieres, 1994, p. 192.
19. Brinks, E., *The Interstellar Medium in Galaxies*, Thronson, H.A., Jr., *et al.*, Eds., Dordrecht: Kluwer, 1990, p. 39.
20. Begeman, K., *Astron. Astrophys.*, 1989, vol. 223, p. 47.
21. Bisnovatyi-Kogan, G.S. and Silich, S.A., *Astron. Zh.*, 1991, vol. 68, p. 749.
22. Silich, S.A., *Astrophys. Space Sci.*, 1992, vol. 195, p. 317.
23. Avedisova, V.S., *Astron. Zh.*, 1971, vol. 48, p. 894.
24. Castor, J., McCray, R., and Weaver, R., *Astrophys. J.*, 1975, vol. 200, p. L107.
25. Weaver, R., McCray, R., Castor, J., *et al., Astrophys. J.*, 1977, vol. 218, p. 377.
26. Gaetz, T.J. and Salpeter, E.E., *Astrophys. J., Suppl. Ser.*, 1983, vol. 52, p. 155.
27. Tomisaka, K. and Ikeuchi, S., *Astrophys. J.*, 1988, vol. 330, p. 695.
28. McCray, R. and Kafatos, M., *Astrophys. J.*, 1987, vol. 317, p. 190.
29. Tenorio-Tagle, G. and Palous, J., *Astron. Astrophys.*, 1987, vol. 186, p. 287.
30. Palous, J., Franco, J., and Tenorio-Tagle, G., *Astron. Astrophys.*, 1990, vol. 227, p. 175.
31. Hudson, D.J., *Statistics, Lectures on Elementary Statistics and Probability*, Geneva, 1964.
32. Arshutkin, L.N. and Kolesnik, I.G., *Stroenie i Evolyutsiya Oblastei Zvezdoobrazovaniya* (Structure and Evolution of Star-Forming Regions), Kiev: Naukova Dumka, 1990, pp. 103 - 160.
33. Karachentsev, I.D., *Astron. Zh.*, 1989, vol. 66, p. 907.